Research Square

Preprints are preliminary reports that have not undergone peer review.
They should not be considered conclusive, used to inform clinical practice,
or referenced by the media as validated information.

Temporal Completeness Reveals Long-Term Hydroclimatic Trend Reversal: A Multi-Temporal Remote Sensing Assessment of Lake Belevi (Türkiye), 2000–2026

Nazif Güler

d250241001@ogr.ikcu.edu.tr

Izmir Kâtip Çelebi University

Müge Ağca

Izmir Kâtip Çelebi University

Zeynel Abidin Polat

Izmir Kâtip Çelebi University

Research Article

Keywords: climate variability, surface water dynamics, satellite monitoring, drought, Google Earth Engine, Mann–Kendall test

Posted Date: August 24th, 2026

DOI: https://doi.org/10.21203/rs.3.rs-10599545/v1

License: This work is licensed under a Creative Commons Attribution 4.0 International License.
Read Full License

Additional Declarations: No competing interests reported.

Temporal Completeness Reveals Long-Term Hydroclimatic Trend Reversal: A Multi-Temporal Remote Sensing Assessment of Lake Belevi (Türkiye), 2000–2026

Nazif Güler [1,*], Müge Ağca [1] and Zeynel Abidin Polat [1]

[1]Department of Geomatics Engineering, İzmir Kâtip Çelebi University, İzmir, Türkiye; d250241001@ogr.ikcu.edu.tr, muge.agca@ikc.edu.tr, zeynelabidin.polat@ikc.edu.tr
*Correspondence: d250241001@ogr.ikcu.edu.tr

Abstract

Climate-induced hydrological change increasingly threatens Mediterranean freshwater systems, yet many satellite-based monitoring studies end before the recent sequence of severe droughts, potentially biasing long-term trend assessments. This study presents a temporally complete 26-year (January 2000–April 2026) hydroclimatic assessment of Lake Belevi (İzmir, Türkiye) using 273 monthly Landsat-derived surface water observations integrated with CHIRPS precipitation, ERA5 temperature, and watershed NDVI within Google Earth Engine. Seasonal Mann–Kendall analysis of the full series revealed a significant decreasing trend ($p = 0.014$, Sen slope = −1.27 ha month^{-1}), whereas the truncated 2000–2020 record showed a significant increasing trend ($p = 0.008$), suggesting that extending observations beyond recent droughts can change the inferred direction of long-term hydrological trends. PELT detection identified five hydrological regime shifts (2005, 2013, 2016, 2022, and 2025), while the 2025 drought reduced lake area to 4.7 ha (96.5% below the 2013–2016 peak), followed by rapid recovery to 180.7 ha by February 2026. Watershed NDVI increased significantly (+53.2%, $p < 0.001$) despite declining water extent. These findings indicate that temporally truncated satellite records may underestimate drought-induced hydrological degradation and even reverse the inferred direction of long-term trends, supporting more robust climate-change attribution and adaptive water-resource management.

Keywords: climate variability; surface water dynamics; satellite monitoring; drought; Google Earth Engine; Mann–Kendall test.

Introduction

Climate change and vulnerability of Mediterranean freshwater systems

Freshwater availability has become one of the most critical environmental challenges of the 21st century due to the combined effects of rising temperatures, altered precipitation regimes, increasing drought frequency, and growing water demand associated with urbanization and agricultural intensification (IPCC, 2013, 2023). Climate change has modified hydrological processes at global and regional scales by increasing hydroclimatic variability, intensifying both extreme precipitation events and prolonged drought periods, and creating substantial pressure on freshwater-dependent ecosystems and societies (Ingrao et al., 2023; Parvaze et al., 2023). Similar challenges have been reported in semi-arid regions, where climate-induced water scarcity increasingly threatens sustainable water-resource management and ecosystem stability (Karimi et al., 2024).

The Mediterranean Basin is among the regions most vulnerable to climate change, with climate projections consistently indicating decreasing precipitation, increasing temperature anomalies, and

prolonged dry seasons under different emission scenarios (IPCC, 2023). Freshwater lakes and reservoirs within this region represent critical components of water-supply systems; however, they are increasingly exposed to compound pressures arising from climate variability, evaporation-driven losses, catchment degradation, and human water demand. Global satellite observations have revealed widespread reductions in lake storage worldwide. Yao et al. (2023) demonstrated that 53% of the world's largest lakes experienced significant water-volume declines between 1992 and 2020, affecting regions inhabited by a substantial proportion of the global population. Similarly, regional studies in Türkiye have documented severe reductions in lake surface area and water levels, including complete desiccation of several lakes in the Göller Yöresi region during recent decades (Işıldar & Ercoşkun, 2021).

The consequences of freshwater decline extend beyond hydrological changes, affecting ecosystem functions, agricultural sustainability, and regional water security. More than 40% of the global population depends directly or indirectly on surface and groundwater resources, particularly in rural and water-limited regions (Sharma et al., 2024). Rapid urban expansion alters land-use patterns and increases pressure on urban environmental resources (Wang & Sun, 2024; Polat et al., 2017). Therefore, reliable long-term monitoring approaches capable of detecting both gradual trends and abrupt hydrological transitions are essential for climate adaptation and sustainable water-resource management. Water scarcity has therefore become a central challenge for sustainable resource management, particularly in regions where increasing climatic variability coincides with rising agricultural and societal water demands (Alotaibi et al., 2023; Ingrao et al., 2023).

Importantly, reliable assessment of long-term hydrological change requires continuous observations capable of capturing emerging climate extremes. Therefore, extending satellite-based records beyond recent anomalies is essential for improving the robustness of climate-impact assessments (IPCC, 2023; Tramblay et al., 2020).

Remote sensing-based monitoring of long-term lake dynamics

Satellite remote sensing provides one of the most consistent approaches for monitoring inland water dynamics over regional to global scales. The Landsat program, with more than five decades of continuous observations at moderate spatial resolution, represents a unique archive for investigating long-term environmental changes (Wulder et al., 2022). Spectral water indices, particularly the Modified Normalized Difference Water Index (MNDWI), have been widely applied for surface water extraction because of their effectiveness in separating open water from surrounding vegetation, soil, and built-up surfaces (Xu, 2006).

The development of cloud-based geospatial platforms, particularly Google Earth Engine (GEE), has further improved the accessibility and reproducibility of multi-decadal satellite analyses by enabling large-scale processing of extensive Earth observation archives (Gorelick et al., 2017). Global products such as the JRC Global Surface Water dataset have significantly advanced understanding of worldwide water dynamics (Pekel et al., 2016). However, global-scale datasets generally cannot fully capture local hydroclimatic variability, seasonal response mechanisms, operational management effects, or abrupt regime shifts occurring within individual managed reservoirs.

Recent studies have demonstrated that lake responses to climate and human pressures vary considerably among regions. Xu et al. (2025) showed that lake-area changes may be controlled primarily by climatic factors in some regions, while anthropogenic influences dominate elsewhere. These findings highlight the need for site-specific, temporally complete assessments capable of identifying local drivers and detecting non-stationary hydrological behavior. Recent investigations further demonstrate that lake-area variations often result from the combined effects of climatic variability and anthropogenic pressures rather than from a single controlling factor (Naeem et al., 2025).

Importantly, the interpretation of long-term hydrological trends depends not only on the availability of satellite archives but also on the temporal completeness of observations. Climate studies end-

ing before recent extreme drought periods may systematically underestimate drought-induced hydrological degradation because newly emerging climate extremes can fundamentally alter the apparent direction of long-term trends (IPCC, 2023; Tramblay et al., 2020).

Research gaps and scientific motivation

Despite substantial progress in satellite-based lake monitoring, two important knowledge gaps remain.

Gap 1 - Influence of temporal completeness on long-term hydrological trend interpretation: Although previous remote sensing studies have successfully quantified long-term lake dynamics (Naeem et al., 2025; Pekel et al., 2016; Yao et al., 2023), relatively few have explicitly examined how extending the observation period beyond recent extreme droughts may alter the statistical interpretation of long-term hydrological trends. Consequently, the implications of temporal incompleteness remain insufficiently explored in Mediterranean freshwater systems.

Gap 2 - Limited understanding of concurrent vegetation dynamics and lake depletion: Vegetation responses to climate change are commonly assessed through satellite-derived vegetation indices such as NDVI. Although vegetation greening and freshwater decline have individually been documented across many regions, their simultaneous occurrence within the same catchment and their implications for water balance remain poorly understood. Increasing vegetation productivity may represent ecosystem recovery in some environments but may also increase evapotranspiration demand in water-limited Mediterranean catchments. Therefore, integrated approaches combining lake dynamics, hydroclimatic variability, drought indicators, and vegetation changes are required to better understand freshwater vulnerability under accelerating climate change.

Unlike previous lake monitoring studies that primarily quantify surface water changes, this study focuses on the methodological implications of temporal completeness by demonstrating how extending observations beyond 2020 alters the inferred direction of long-term hydrological trends. Furthermore, the study integrates change-point detection, lagged hydroclimatic analysis, SPI-based drought characterization, and vegetation dynamics into a unified framework for Mediterranean freshwater monitoring.

Study objectives and contributions

This study investigates the long-term hydroclimatic evolution of Lake Belevi, a Mediterranean freshwater reservoir in western Türkiye, using a temporally complete Landsat-based monitoring framework covering January 2000–April 2026. Rather than focusing solely on local lake-area change, the study aims to demonstrate how temporal completeness influences the interpretation of climate-driven hydrological trends.

The specific contributions of this study are: (1) providing a 273-month continuous Landsat-based assessment of Lake Belevi (2000–2026); (2) demonstrating statistically verified reversal of long-term trend direction when observations are extended beyond 2020; (3) integrating Seasonal Mann–Kendall analysis, PELT change-point detection, SPI-3 drought characterization, lagged hydroclimatic analysis, and vegetation dynamics within a unified monitoring framework; (4) developing a workflow, demonstrated for Lake Belevi, that is in principle applicable to long-term monitoring of other Mediterranean freshwater systems under accelerating climate change; and (5) demonstrating the implications of temporal non-stationarity for adaptive water-resource planning and climate-impact assessment.

Materials and methods

Study area

Lake Belevi is a shallow freshwater reservoir located in western Türkiye within the Küçük Menderes Basin, approximately 53 km southeast of İzmir city center (38°01′24.9″N, 27°27′59.6″E). Based on

epoch-based measurements obtained on 22 April 2026 through the TUSAGA-Active (CORS-TR) system of the General Directorate of Land Registry and Cadastre (Tapu ve Kadastro Genel Müdürlüğü), the elevation of Lake Belevi was determined to be 5.17 m. The lake is situated within the alluvial plain of the Küçük Menderes River system and currently functions as an important municipal freshwater resource for Tire and Selçuk districts. Its location within the Mediterranean climatic zone makes Lake Belevi particularly sensitive to changes in precipitation variability, temperature increase, and drought intensification.

The region experiences a typical Mediterranean climate (Köppen–Geiger classification: Csa), characterized by hot and dry summers and mild, precipitation-dominated winters. Annual precipitation is approximately 750 mm, with the majority occurring between October and April, whereas summer months receive minimal rainfall. This pronounced seasonal hydroclimatic pattern creates strong dependence of lake storage on winter precipitation accumulation and subsequent evaporative losses during the dry season. ERA5-derived mean annual temperature during the reliable 2005–2020 period was 17.6 °C, consistent with regional climatological conditions.

Lake Belevi represents an appropriate case study for investigating temporal non-stationarity in Mediterranean freshwater systems because its hydrological evolution during the satellite observation period includes contrasting wet and dry phases. The lake experienced relatively high storage conditions during the 2013–2016 period, followed by progressive depletion and an extreme drought-induced reduction in surface water extent during 2025. The subsequent rapid refilling observed in early 2026 provides a unique opportunity to examine how recent climate extremes influence the interpretation of long-term hydrological trends. Therefore, the lake provides an effective natural laboratory for assessing whether incomplete satellite records may bias the detection of long-term hydroclimatic changes.

Historically, Lake Belevi was drained and converted into agricultural land during the 1940s but was re-established as a lake in 1992 following embankment construction associated with the İzmir–Aydın highway. The reservoir has a maximum surface area of approximately 305 ha at full capacity. During the 273-month Landsat observation period (January 2000–April 2026), detected surface water extent varied from 1.1 ha to 276.7 ha, demonstrating substantial intra- and inter-annual variability suitable for satellite-based hydroclimatic assessment. Surrounding areas consist mainly of agricultural land, reed beds, and Mediterranean shrub vegetation, providing an appropriate environment for evaluating concurrent changes in surface water dynamics and watershed vegetation conditions.

Landsat data collection and pre-processing

Multi-temporal Landsat imagery was obtained from the USGS Collection 2 Tier 1 Level-2 surface reflectance archive through the Google Earth Engine (GEE) platform. Four Landsat missions were integrated: Landsat 5 TM (2000–2013), Landsat 7 ETM+ (2000–2022), Landsat 8 OLI (2013–2026), and Landsat 9 OLI-2 (2021–2026), providing a continuous moderate-resolution satellite record for long-term hydroclimatic assessment. Cloud and cloud-shadow contamination were removed using the QA_PIXEL quality assessment band, and Collection 2 surface reflectance scaling factors were applied. Spectrally consistent bands (Green, Red, NIR, and SWIR1) were harmonized among sensors, and monthly median composites were generated from all available cloud-free observations. For 2026, only January–April observations were included to avoid incomplete-year bias.

MNDWI computation and threshold validation

MNDWI was computed as (Green − SWIR1) / (Green + SWIR1) following Xu (2006), with a classification threshold of 0.1 to identify water pixels. The threshold was determined through sensitivity analysis using Sentinel-2 Surface Reflectance imagery (15 validation scenes, 2017–2024) representing different hydrological conditions to minimize false-positive classification of moist soil and urban surfaces while retaining open water at depths detectable by 30 m resolution imagery. A representative surface water classification map derived from Sentinel-2 imagery is shown in Figure 1 to illustrate the

spatial pattern of MNDWI-based water detection at the lake. Surface water area (ha) was derived by aggregating water pixel areas (900 m²/pixel) within the AOI. Monthly observations were filtered to retain values between 1 ha (minimum detectable extent given pixel size and mixed-pixel effects) and 350 ha (physical upper bound above maximum lake capacity), yielding 273 valid monthly observations.

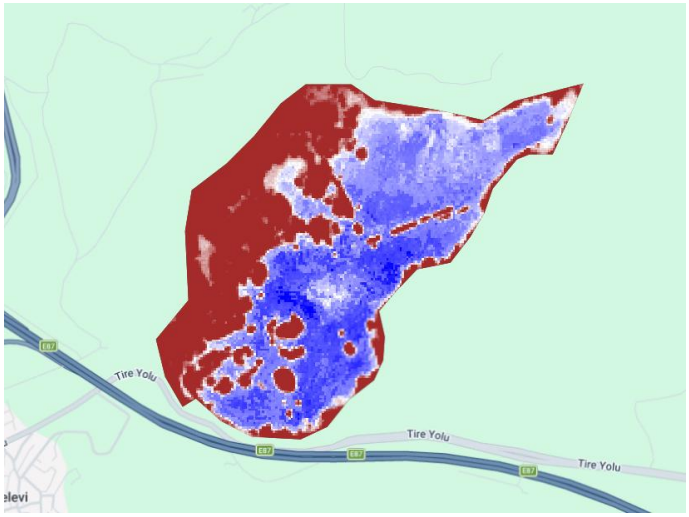


Fig. 1 Landsat-derived surface water map of Lake Belevi (2023). Blue pixels indicate MNDWI > 0.1 (open water); red pixels indicate non-water surfaces. This GEE-generated visualization illustrates the spatial heterogeneity of water extent detection and the utility of spectral water indices for lake monitoring

Table 1. MNDWI threshold sensitivity analysis results based on Sentinel-2 reference validation (15 scenes, 2017–2024). The threshold of 0.10 was selected because it provided a suitable compromise between Producer's Accuracy and User's Accuracy while maintaining high overall classification accuracy.

Threshold	n Validation Scenes	Overall Accuracy	Kappa	Producer's Acc. (Water)	User's Acc. (Water)
0.00	15	96.35%	0.8733	91.83%	87.92%
0.05	15	96.35%	0.8722	89.90%	89.52%
0.10*	15	96.29%	0.8684	87.73%	91.00%
0.15	15	96.06%	0.8573	84.89%	92.20%
0.20	15	95.72%	0.8399	81.54%	93.31%

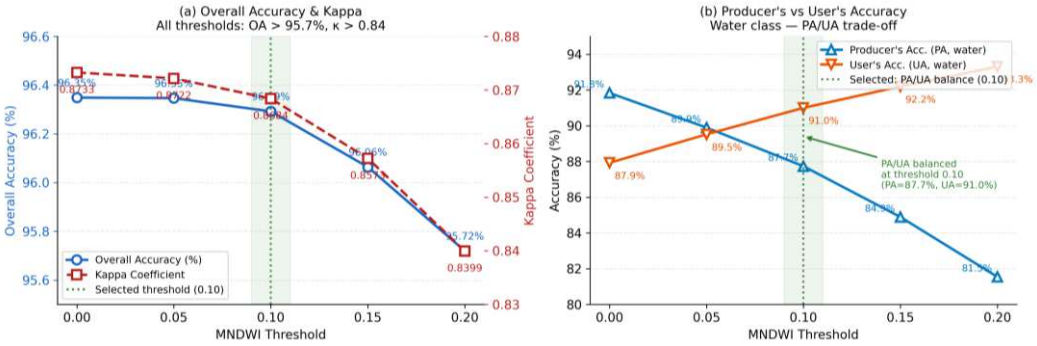


Fig. 2 MNDWI threshold sensitivity analysis based on Sentinel-2 SR reference classification (n = 15 validation scenes, 2017–2024, high- and medium-water conditions). (a) Overall accuracy and Kappa coefficient across five candidate thresholds. All thresholds yielded OA > 95.7% and κ > 0.84. (b) Trade-off between Producer's Accuracy (PA) and User's Accuracy (UA) for the water class. Threshold 0.10 (vertical dotted line) was selected as it best

balances PA (87.7%) and UA (91.0%), minimising false positive water classifications from moist soils while retaining open water detection. The marginal OA difference between 0.00 and 0.10 is 0.06%, confirming threshold robustness

Hydroclimatic data and watershed NDVI

Monthly precipitation data were obtained from CHIRPS (Funk et al., 2015) and spatially averaged over the watershed area to represent catchment-scale rainfall variability. Monthly mean air temperature was obtained from ERA5 reanalysis (Hersbach et al., 2020). ERA5 temperature values for 2000–2004 were compared against regional climatological averages and showed unrealistic discontinuities; therefore, these years were excluded from temperature-dependent analyses. Temperature-based analyses were consequently conducted for the period with consistent data availability (2005–2020), while precipitation-based analyses covered the complete observation period. A 3-month Standardized Precipitation Index (SPI-3) was calculated to characterize cumulative drought conditions.

Annual watershed-scale NDVI was computed from Landsat median composites restricted to the March–October growing season (Mediterranean climate vegetation period) and spatially averaged over the watershed boundary at 30 m resolution, generating a 27-year record (2000–2026). The partial-year 2026 value (8 scenes) is excluded from trend analysis; the valid NDVI trend series spans 2000–2025 (n = 26).

Statistical methods: rationale and selection criteria

The selection of statistical methods was guided by the specific characteristics of the monthly surface water area time series, including non-normal distribution, strong seasonal variability (12-month periodicity), temporal dependence, and the need to identify both gradual monotonic changes and abrupt regime shifts. Therefore, a combination of non-parametric trend analysis, robust slope estimation, change-point detection, and hydroclimatic association analyses was applied. The statistical approaches and their methodological rationales are summarized in Table 2.

Table 2. Statistical Methods Applied in This Study and Their Selection Rationale

Method	Properties	Why Selected for This Study	Alternative Considered	Reference
Seasonal Mann-Kendall Test	Non-parametric; robust to non-normality and autocorrelation; handles seasonal periodicity (period=12)	Monthly water area series is non-normal, seasonally structured (Mediterranean cycle). Parametric OLS trend would be invalid due to seasonal autocorrelation.	Linear regression (rejected: assumes normality, no seasonality)	(Hirsch & Slack, 1984)
Mann-Kendall Test (annual/NDVI)	Non-parametric monotonic trend test; distribution-free	Annual means and NDVI series are small samples (n ≤ 27) with potential non-normality. Standard t-test for trend invalid.	Pearson correlation (rejected: normality assumption)	(Kendall & Gibbons, 1962; Mann, 1945)
Sen's Slope Estimator	Median-based slope; robust to outliers	Lake water area contains anomalous years (2001 outlier: 5.3 ha). Median-based slope is more reliable than mean-based OLS slope.	OLS slope (rejected: sensitive to outliers)	(Sen, 1968)

PELT Change-Point Detection	Optimal exact change-point detection; O(n) computational cost; penalized likelihood approach	The lake exhibits multiple regime shifts (not just one), requiring detection of 5 breakpoints. PELT handles multiple change-points efficiently; CUSUM limited to single change-point.	CUSUM (rejected: single change-point only)	(Killick et al., 2012)
Kruskal-Wallis & Mann-Whitney U	Non-parametric multi-group and pairwise comparison; no normality assumption	Comparing water area distributions across PELT segments; segments have unequal variances (Levene test: $p < 0.05$) and non-normal distributions.	ANOVA (rejected: normality and homoscedasticity violated)	(Kruskal & Wallis, 1952)
Lagged cross-correlation (Pearson r)	Linear association quantification at specified time lags	Physically motivated lag structure (catchment routing time: 2–4 months). Pearson r used as a first-order linear approximation; Spearman r used as robustness check for NDVI.	Spearman r (used as robustness check for NDVI)	(Chatfield & Xing, 2019)
Multivariate OLS Regression	Simultaneous estimation of multiple predictor contributions; interpretable standardized coefficients	Quantify relative contributions of lag3_rain, lag2_temp, and NDVI. Standardized coefficients enable direct comparison of predictor importance. Machine learning methods (RF, LSTM) deferred to future work.	Random Forest (deferred: requires larger training set and external validation)	(Draper & Smith, 1998)

The statistical framework applied in this study was designed to address the specific characteristics of long-term hydroclimatic time series, including seasonal variability, non-normal distributions, potential temporal dependence, and abrupt regime transitions. Accordingly, non-parametric trend analysis (Seasonal Mann–Kendall and Mann–Kendall tests) was used to identify monotonic changes, while Sen's slope estimation quantified the magnitude of detected trends. PELT change-point detection was applied to identify structural transitions within the long-term water-area series, and lagged correlation analysis was performed to evaluate delayed responses between hydroclimatic drivers and reservoir dynamics. Finally, multivariate OLS regression was used to quantify the combined contribution of climatic and ecological predictors to observed water-area variability.

Results and discussion

Monthly surface water area: full 2000–2026 time series

Monthly surface water area at Lake Belevi ranged from 1.1 ha (October 2003) to 276.7 ha across the full observation period, with a 273-month mean of 107.2 ha (SD = 48.2 ha). Clear seasonal cycles are evident, with higher water extents in late winter and spring (February–April) and minimum values in late summer and autumn (August–October), consistent with Mediterranean hydrological seasonality.

The Seasonal Mann–Kendall analysis of the complete 2000–2026 record indicated a significant decreasing trend ($p = 0.014$, Tau = −0.107, Sen slope = −1.27 ha month^{-1}). In contrast, analysis of the truncated 2000–2020 period resulted in a significant increasing trend ($p = 0.008$, Tau = +0.138, Sen slope = +1.90 ha month^{-1}). This difference indicates that extending the observation period beyond 2020 changes the direction of the inferred long-term trend, highlighting the sensitivity of lake trend estimates to temporal completeness.

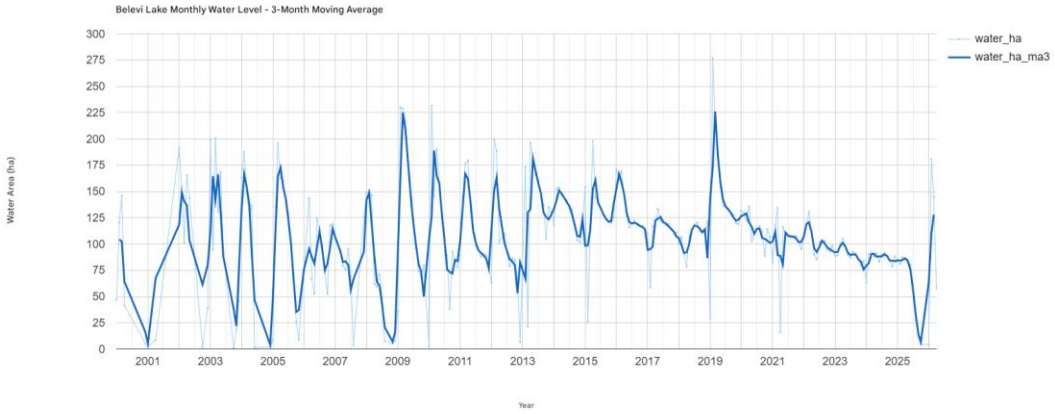


Fig. 3 Monthly surface water area of Lake Belevi (January 2000 – April 2026; n = 273) with 3-month moving average

Annual mean surface water area and trend

Annual mean water area showed no significant monotonic trend over the full 27-year record (MK $p = 0.933$, Tau = 0.014), indicating a multi-phase temporal evolution rather than a monotonic annual pattern: increasing through 2013–2019 and declining through 2020–2026. The 2001 annual mean (5.3 ha) is anomalously low, attributed to limited cloud-free Landsat availability in that year rather than actual lake desiccation.

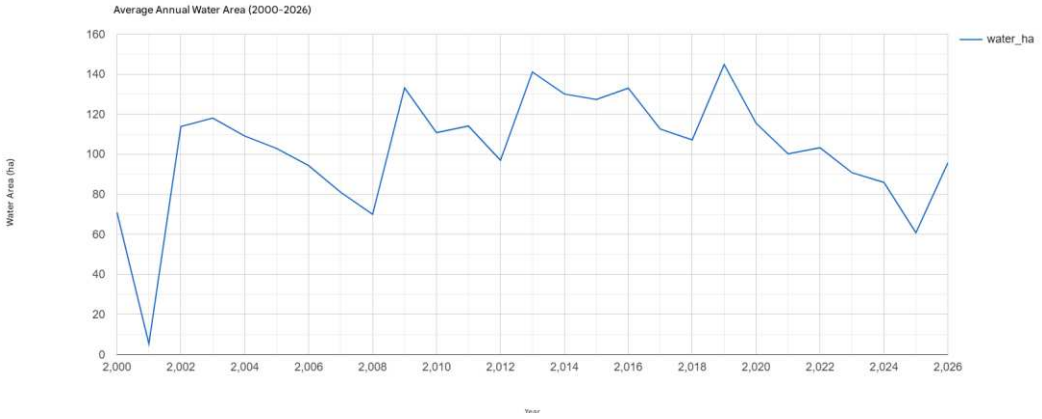


Fig. 4 Annual mean surface water area of Lake Belevi (2000–2026). Mann-Kendall: $p = 0.933$ (no significant monotonic trend)

Hydroclimatic variability during the observation period

Monthly precipitation exhibited substantial interannual variability during the observation period, with a decreasing tendency during the early 2000s followed by pronounced fluctuations after 2007 (Figure 5). Mean monthly precipitation was 64.9 mm, indicating considerable variability in water availability throughout the record. ERA5 temperature data showed a general warming tendency between 2000 and 2020 (Figure 6), although the first five years were excluded from temperature-dependent analyses because of reliability constraints. These hydroclimatic variations provide the climatic context for the observed changes in reservoir storage and drought-related fluctuations.

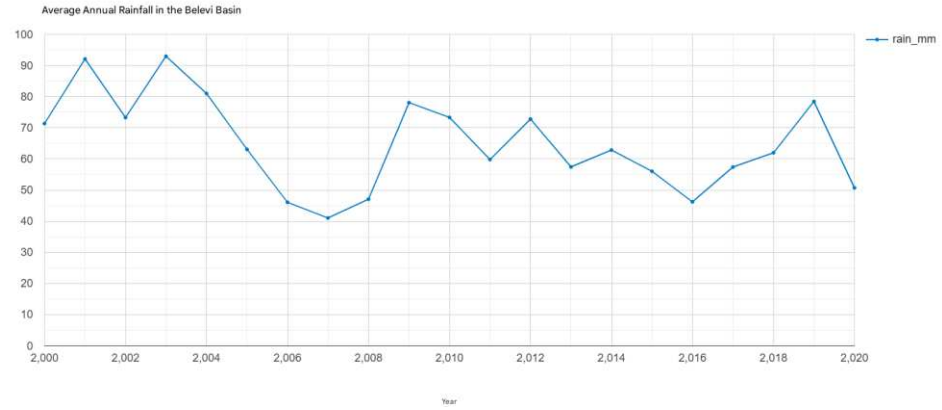


Fig. 5 Annual mean monthly precipitation from CHIRPS (2000–2020). Mean = 64.9 mm/month

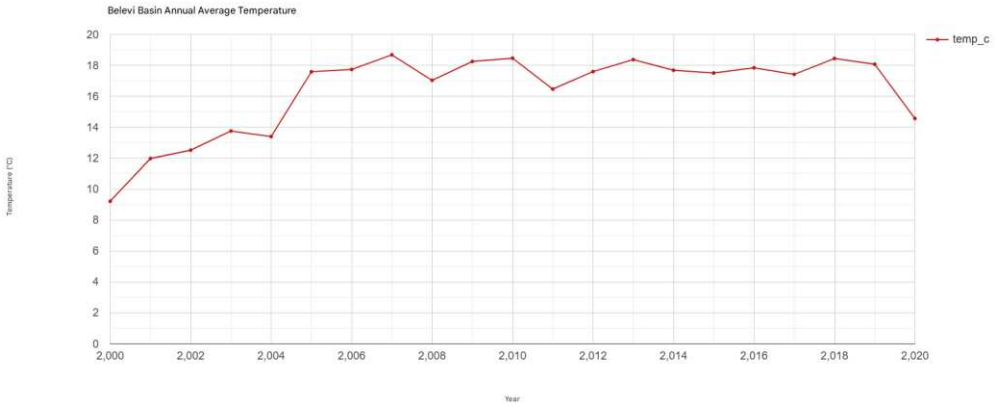


Fig. 6 Annual mean 2-meter air temperature from ERA5 (2000–2020)

PELT structural change-point analysis

PELT analysis of the full 273-month series identified five breakpoints at 2005, 2013, 2016, 2022, and 2025, delineating six distinct water-area regimes (Table 3; Figure 3). Mean water area describes a rise–peak–decline trajectory: 101.4 ha (2000–2005), 102.3 ha (2005–2013), 134.8 ha (2013–2016, peak segment), 115.8 ha (2016–2022), 89.1 ha (2022–2025, pre-drought), and 61.6 ha (2025–2026, drought/refill partial year). Kruskal-Wallis confirmed highly significant differences among segments ($H = 48.43$, $p < 0.001$). Pairwise tests indicated the 2013–2016 peak segment differed from 2005–2013 ($p = 0.0001$) and 2016–2022 ($p < 0.001$). The 2022–2025 pre-drought segment differed significantly from all preceding periods (all $p < 0.05$).

Table 3. Water-area regime segments identified by PELT change-point analysis (2000–2026)

Segment	n (months)	Mean (ha)	SD (ha)	Trend (slope)	Hydrological Interpretation
2000–2005	35	101.4	71.4	+1.117 ha/mo (ns) [a]	High variability; L5/L7 SLC-off transition
2005–2013	85	102.3	55.5	+0.351 ha/mo (ns) [a]	Stable period; L8 onset (2013)
2013–2016	35	134.8	28.4	−0.122 ha/mo (ns) [a]	Peak storage; wet regional conditions
2016–2022	75	115.8	31.6	Moderate	Gradual declining phase; warming trend

2022–2025	35	89.1	8.0	Declining	Pre-drought depletion; lowest variability
2025–2026	8	61.6	66.9	Extreme	Extreme variability period associated with the 2025 low-water event and subsequent 2026 recovery

[a] ns = not significant ($p > 0.05$). SD = standard deviation. All trend slopes in ha/month.

Watershed NDVI: sustained greening trend

Annual watershed NDVI increased significantly between 2000 and 2025 (MK $p < 0.001$, Tau = 0.680, Sen slope = +0.00457/yr; Figure 7). NDVI increased from 0.308 in 2000 to 0.472 in 2025, a relative increase of 53.2%, with the 2026 partial-year value (0.367; only 8 scenes) likely underestimating actual growing-season NDVI and excluded from trend analysis. This sustained greening pattern is consistent with previously reported vegetation recovery trends in Mediterranean ecosystems (Zhu et al., 2016).

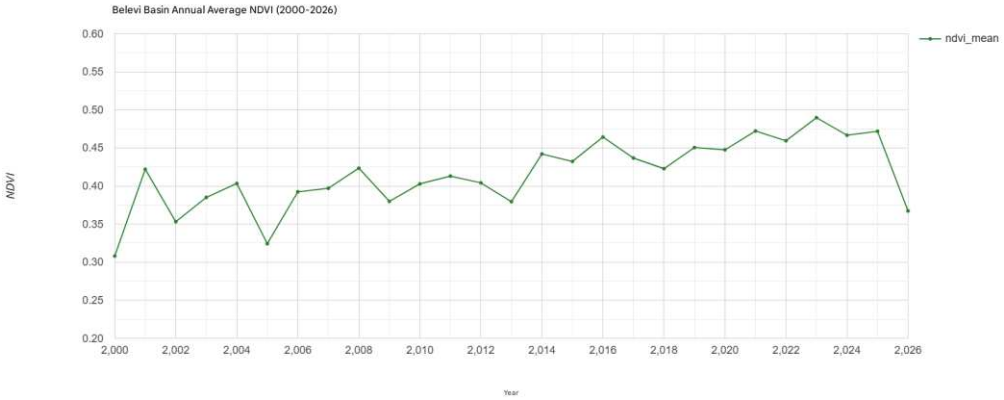


Fig. 7 Annual mean NDVI of the Belevi watershed (2000–2026; March–October growing season)

Seasonal hydroclimatic correlation

The seasonal decomposition of precipitation–water area and temperature–water area correlations (Figure 8) reveals a marked asymmetry across the four seasons of the Mediterranean hydrological year. The strongest positive precipitation signal occurs in summer ($r = 0.235$), when antecedent wet-season storage determines how far the reservoir has depleted by peak evaporative demand in July–August. Winter ($r = -0.128$) and autumn ($r = -0.170$) show weakly negative or negligible precipitation correlations, suggesting that concurrent seasonal precipitation alone does not fully explain reservoir storage variability.

Temperature exerts its strongest suppressive effect in spring ($r = -0.201$) and summer ($r = -0.255$), seasons when elevated evapotranspiration from the catchment and direct open-water evaporation reduce net inflow to the reservoir. The positive autumn temperature correlation ($r = +0.172$) likely reflects the lagged influence of the preceding wet winter: years with higher winter rainfall produce higher spring temperatures through reduced cloud cover and albedo effects, while simultaneously sustaining higher reservoir storage into the autumn. This cross-seasonal dependency highlights the importance of interpreting seasonal correlations within the broader lagged hydroclimatic framework developed in Section 4.7, rather than as direct causal relationships between concurrent meteorological and hydrological variables.

Taken together, the seasonal patterns are consistent with the Mediterranean's characteristic summer-dominant evaporative control and winter-dominant precipitation recharge regime (Jiménez-

Bonilla et al., 2023; Pınarlık et al., 2023), and suggest that the most critical period for reservoir management interventions is the spring transition, when temperature-driven depletion begins to outpace any residual wet-season inflows.

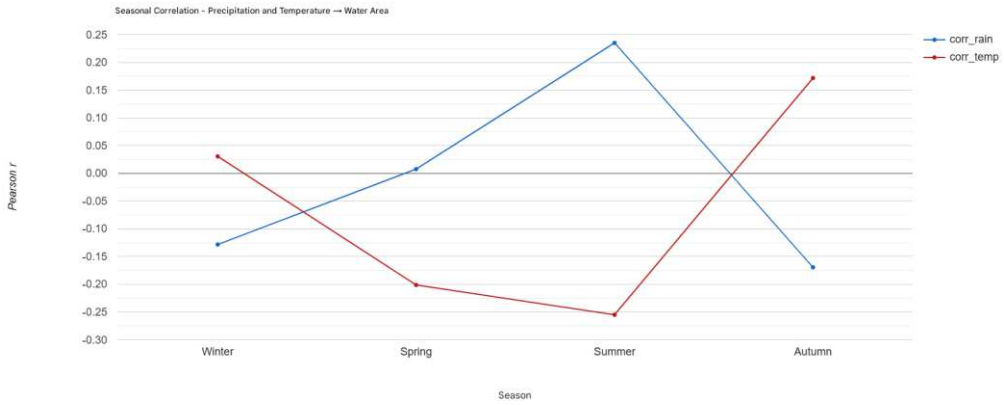


Fig. 8 Seasonal correlation coefficients between precipitation (blue) and temperature (red) and lake water area across the four seasons

Lagged hydroclimatic controls

Precipitation exerted its peak positive influence at a 3-month lag (r = 0.404; Figure 9), with positive correlations sustained from lag-1 (r = 0.353) through lag-4 (r = 0.345). The near-zero lag-0 correlation (r = −0.066) reflects MNDWI suppression during active rainfall events due to suspended sediment turbidity. Temperature showed maximum suppressive effect at lag-2 (r = −0.414; Figure 10), consistent with a 2-month evapotranspiration-driven depletion mechanism, declining toward zero by lag-6.

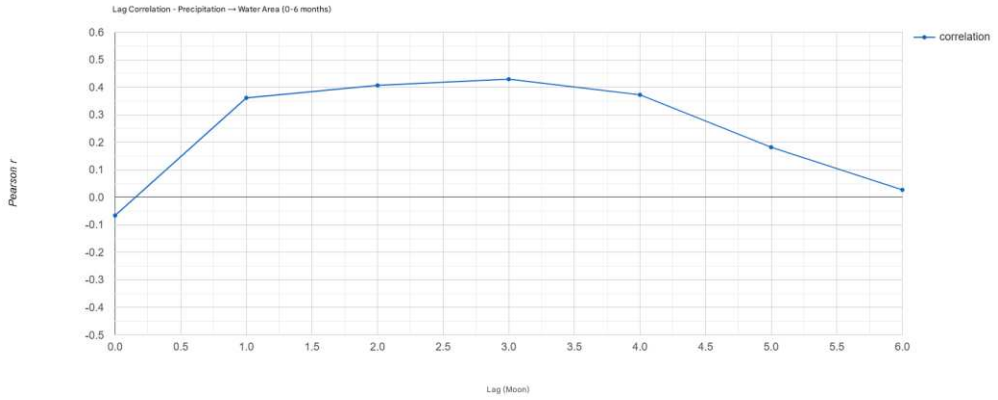


Fig. 9 Lag-correlation between monthly precipitation and surface water area (lag 0–6 months; 2000–2026). Peak positive correlation at lag-3 (r = 0.404)

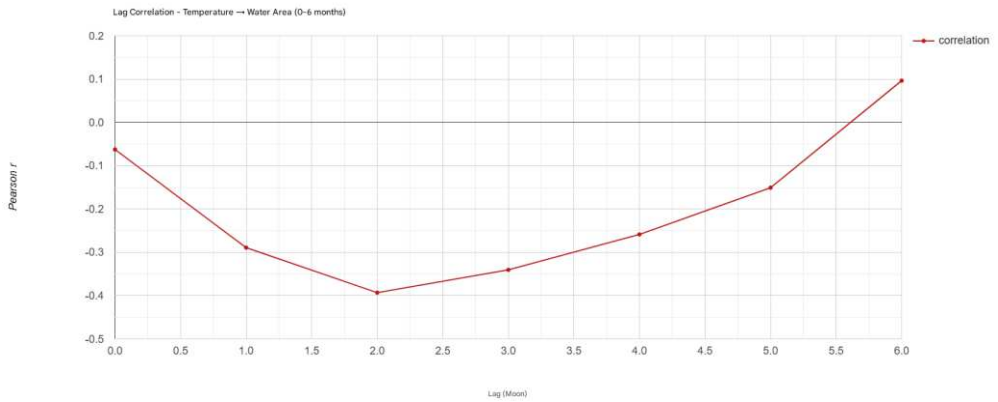


Fig. 10 Lag-correlation between monthly mean temperature and surface water area (lag 0–6 months; ERA5 period 2005–2020)

The 2025 extreme drought event and 2026 rapid refilling

The 2025 drought represents the most severe water stress event recorded at Belevi in the 26-year satellite record, supported by publicly available photographic evidence from November 2025 (TRT Haber, 2025). Surface water area declined from 87.5 ha in March 2025 to 79.9 ha (June), 61.2 ha (July), 27.9 ha (August), 11.0 ha (September), and a nadir of 4.7 ha in October 2025 — a 96.5% reduction from the 2013–2016 peak mean. The 2005–2019 and 2023 satellite image overlay visually documents this progressive retreat. The rapid refilling to 180.7 ha in February 2026 — approximately 44 times larger than the January 2026 value — reflects exceptional late-winter precipitation following the 2025 drought, demonstrating the alternating drought-deluge dynamics increasingly characteristic of Mediterranean climate change scenarios. This recovery is further corroborated by a field photograph taken on 23 April 2026, which shows extensive open water and reed regrowth across the basin (Fig. 11).



Fig. 11 Ground-level view of Lake Belevi on 23 April 2026 (14:14 local time), showing extensive open water and dense reed (Phragmites) stands consistent with the rapid post-drought recovery documented in the satellite record. Photograph by the authors.

Multivariate regression analysis (ERA5 period: 2005–2020)

To evaluate the relative contribution of climatic and ecological variables to monthly surface water variability, two sequential OLS regression models were developed using the ERA5-reliable period (2005–2020), during which temperature observations were considered suitable for hydroclimatic analysis (Section 3.3).

Model 1 included lag-3 precipitation, lag-2 temperature, and annual NDVI as explanatory variables ($n = 172$). The model explained 23.6% of monthly water-area variability ($R^2 = 0.236$, adjusted $R^2 = 0.222$), with prediction errors of MAE = 30.8 ha and RMSE = 40.9 ha. Among the predictors, lag-3 precipitation represented the strongest positive contribution (standardized $\beta = 15.68$, $p < 0.001$), indicating that antecedent precipitation conditions were associated with increased subsequent reservoir water extent. Lag-2 temperature showed a negative effect ($\beta = -8.51$, $p = 0.050$), suggesting a potential suppressive influence of elevated thermal conditions, whereas NDVI showed a significant positive relationship with water-area variability ($\beta = 8.49$, $p = 0.011$).

Model 2 incorporated lag-3 SPI-3 to represent cumulative precipitation anomalies and drought conditions beyond monthly rainfall variability. The addition of SPI-3 increased the explained variance

from 23.6% to 26.9% (R^2 = 0.269, adjusted R^2 = 0.252) and slightly improved model performance (MAE = 29.3 ha; RMSE = 39.8 ha). The improved model performance indicates that cumulative drought conditions provide additional information for explaining reservoir storage variability beyond individual precipitation and temperature variables.

Although the regression models explained a meaningful proportion of the observed variability, a considerable amount of variance remained unexplained (73.1% in Model 2). This residual variability may reflect additional processes not represented in the current framework, including reservoir operation practices, water-use dynamics, groundwater interactions, and other catchment-scale factors. Quantitative assessment of these factors was beyond the scope of this study because consistent operational datasets covering the entire observation period were unavailable.

Table 4. Summary of All Statistical Results (January 2000 – April 2026)

Analysis	Dataset / Period	Result	p-value	Significance / Note
Seasonal MK — Monthly Water Area	2000–2026 (n=273)	↓ Decreasing, −1.27 ha/mo	0.014	* (contrasts 2000-2020 sub-period)
Annual MK — Water Area	2000–2026 (n=27)	No trend	0.933	ns
NDVI MK — Watershed	2000–2025 (n=26)	↑ Increasing, +0.00457/yr	< 0.001	*** (+53.2% total)
PELT Breakpoints	Monthly series	2005, 2013, 2016, 2022, 2025	—	K-W H=48.43, p<0.001
Period Mean 2013–2016 (peak)	Monthly water area	134.8 ha	—	Highest of all segments
Period Mean 2022–2025	Monthly water area	89.1 ha	< 0.05 vs 2013-16	−33.9% vs peak segment
Oct 2025 drought minimum	2025 event	4.7 ha	—	96.5% decline from 2013-16 mean
Feb 2026 refill maximum	2026 event	180.7 ha	—	44-fold increase from Jan 2026
NDVI × Water Area (Pearson)	Annual (n=21)	r = 0.218	0.343	ns (bivariate)
Lag Precipitation (peak lag=3)	2000–2026 monthly	r = 0.404	—	3-month catchment lag
Lag Temperature (peak lag=2)	ERA5 2005–2020	r = −0.414	—	2-month ET suppression
Model 1 OLS	2005–2020 (n=172)	R^2 = 0.236	—	MAE=30.8 ha, RMSE=40.9 ha
Model 2 OLS (+SPI-3)	2005–2020 (n=171)	R^2 = 0.269	—	MAE=29.3 ha, RMSE=39.8 ha
β lag3_rain (std.)	Regression	+15.68	< 0.001	*** dominant predictor
β lag2_temp (std.)	Regression	−8.51	0.050	* suppressive effect
β NDVI (std.)	Regression	+8.49	0.011	* positive partial effect

Significance: * p < 0.05; ** p < 0.01; *** p < 0.001; ns: not significant. MK = Mann-Kendall; K-W = Kruskal-Wallis; std. = standardized.

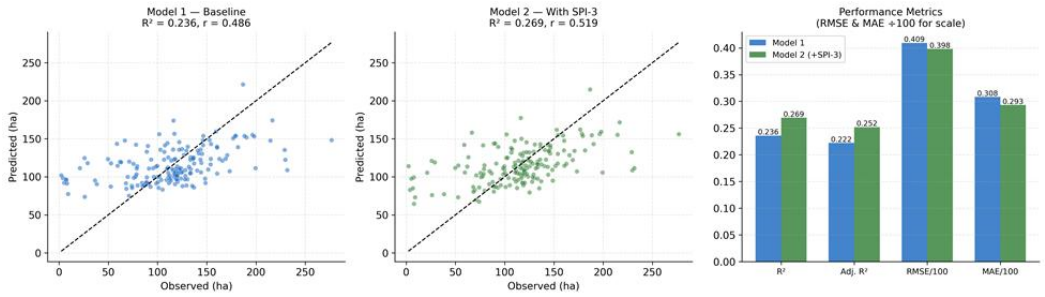
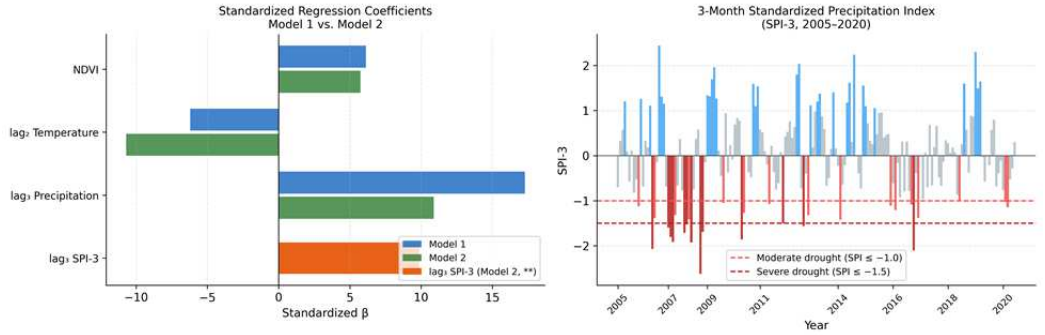


Fig. 12 OLS Regression Model Comparison (2005–2020 ERA5 Period). (a) Model 1 (lag_3 precipitation + lag_2 temperature + NDVI): $R^2 = 0.236$, MAE = 30.8 ha. (b) Model 2 (+ SPI-3): $R^2 = 0.269$, MAE = 29.3 ha. (c) Performance metric comparison. The addition of SPI-3 improved explained variance by 3.4 percentage points



(**a**) (**b**)

Fig. 13 (a) Standardized regression coefficients (β) for Model 1 and Model 2. SPI-3 (orange) is significant at p = 0.004 (**). (b) SPI-3 time series (2005–2020) showing drought classification thresholds. Red bars indicate moderate to severe drought months (SPI-3 ≤ −1.0)

Temporal completeness and the detection of long-term trend reversal

A major finding of this study is that the interpretation of Lake Belevi's long-term hydrological trajectory is highly sensitive to the temporal extent of the observation period. When the analysis was restricted to the 2000–2020 period, the Seasonal Mann–Kendall test indicated a significant increasing trend in surface water area (p = 0.008, Tau = +0.138, Sen slope = +1.90 ha $month^{-1}$). However, extending the record to include the recent 2021–2026 period resulted in a statistically significant decreasing trend (p = 0.014, Tau = −0.107, Sen slope = −1.27 ha $month^{-1}$). This reversal demonstrates that incomplete temporal coverage can substantially alter the interpretation of hydroclimatic trends, particularly in Mediterranean environments characterized by strong interannual variability and episodic extreme events.

The recent decline observed after 2020 coincides with a period of intensified drought conditions across the eastern Mediterranean region, where increasing temperatures and decreasing precipitation trends have been widely reported under climate change scenarios (IPCC, 2023; Tramblay et al., 2020). Therefore, studies based solely on historical periods ending before recent extreme events may underestimate emerging water stress signals. The results highlight the importance of maintaining long-term continuous observations when evaluating freshwater system responses under non-stationary climate conditions.

The PELT change-point analysis further supports this interpretation by demonstrating that Lake Belevi did not follow a simple monotonic trajectory but instead experienced multiple transitions between distinct hydrological regimes. The identified breakpoints (2005, 2013, 2016, 2022, and 2025) indicate alternating phases of relative stability, increased water storage, gradual depletion, and extreme

drought. Some breakpoints coincide with periods of Landsat sensor transition, particularly the introduction of Landsat 8 in 2013. Although the use of Collection 2 surface reflectance products and sensor harmonization minimizes potential inter-sensor radiometric differences, minor sensor-related influences cannot be completely excluded. Nevertheless, the persistence of statistically distinct hydrological regimes, together with their agreement with observed hydroclimatic variability, suggests that the detected transitions primarily represent real environmental change rather than sensor-related artefacts.

Although derived from a single case study, our findings raise a broader methodological concern for long-term hydroclimatic monitoring. Numerous satellite-based lake studies published before 2021 necessarily exclude the recent sequence of extreme Mediterranean droughts. Our results suggest that such temporal truncation may not merely underestimate the magnitude of hydrological degradation but may also reverse the inferred direction of long-term trends — a hypothesis that warrants testing across a broader sample of Mediterranean lakes.

The 2025 drought event and increasing hydroclimatic extremes

The 2025 drought represents the most severe water reduction event detected within the Landsat observation period. Surface water area declined from the 2013–2016 peak regime mean of 134.8 ha to only 4.7 ha in October 2025, corresponding to a 96.5% reduction. This extreme reduction is consistent with increasing drought intensity reported across Mediterranean freshwater systems, where higher evaporative demand and prolonged precipitation deficits are altering lake hydrological stability (Jiménez-Bonilla et al., 2023; Pınarlık et al., 2023). Similar climate-driven pressures on surface water resources have been reported in other water-limited regions, demonstrating the broader relevance of drought-induced hydrological vulnerability (Ray & Tikuye, 2025).

Independent visual evidence from November 2025 panoramic imagery supports the satellite-derived observation of near-complete lake surface reduction. The agreement between remote sensing estimates and external observations increases confidence in the capability of MNDWI-based monitoring for detecting extreme hydrological transitions.

Conversely, the rapid increase in water extent observed in early 2026, reaching 180.7 ha in February 2026, illustrates the increasing importance of compound hydroclimatic extremes in Mediterranean regions. Such rapid transitions between drought conditions and sudden recovery events may create additional challenges for reservoir management because short-term recovery does not necessarily indicate long-term hydrological stabilization.

NDVI–water relationship and the complexity of catchment responses

The simultaneous increase in watershed NDVI (+53.2% between 2000 and 2025) and the long-term decline in surface water availability reveals a complex relationship between vegetation dynamics and hydrological response. This finding challenges the assumption that increasing vegetation productivity necessarily represents improved catchment water availability, particularly in Mediterranean environments where water limitation strongly regulates ecosystem processes. Similar ecological responses have demonstrated that vegetation dynamics under climate change do not necessarily indicate enhanced ecosystem resilience, as vegetation productivity may be constrained by increasing climatic stress and water limitations (Anderegg et al., 2020).

The positive NDVI coefficient obtained from the regression model ($\beta = +8.49$, $p = 0.011$) should be interpreted cautiously. Rather than indicating a direct causal effect of vegetation increase on reservoir storage, this relationship likely reflects the co-occurrence of higher vegetation productivity and favourable hydroclimatic conditions during relatively wet periods. In water-limited Mediterranean catchments, vegetation expansion may provide ecological benefits while simultaneously increasing ecosystem water demand through enhanced evapotranspiration processes.

Therefore, the observed NDVI–water divergence suggests that vegetation indices alone are insufficient indicators of catchment water availability. Integrated assessments combining vegetation dynamics with evapotranspiration, soil moisture, groundwater conditions, and precipitation variability are required to better understand vegetation–water interactions. Future studies incorporating dedicated evapotranspiration products, such as MODIS MOD16 or ERA5-Land evaporation datasets, could provide further insights into the mechanisms controlling water balance changes in Mediterranean freshwater catchments.

Hydroclimatic drivers and implications for sustainable water management

The lagged correlation analysis demonstrated that precipitation and temperature influence Lake Belevi with delayed responses rather than immediate effects. Precipitation showed the strongest relationship with water area at a 3-month lag ($r = 0.404$), indicating the importance of antecedent rainfall accumulation within the catchment. Similarly, temperature exhibited its strongest negative association at a 2-month lag ($r = -0.414$), consistent with delayed effects of enhanced evapotranspiration and catchment water loss.

The regression models further supported the importance of cumulative hydroclimatic conditions. The inclusion of SPI-3 improved model performance from $R^2 = 0.236$ to $R^2 = 0.269$, indicating that drought accumulation provides additional explanatory information beyond monthly precipitation alone. However, the remaining unexplained variability indicates that climatic factors alone cannot fully describe reservoir dynamics.

Lake systems are influenced not only by climate but also by operational decisions, water demand, groundwater interactions, and catchment management practices. These factors were not included in the current modelling framework due to the absence of consistent long-term operational datasets. Therefore, the results should be interpreted as identifying major hydroclimatic controls rather than providing a complete attribution of all processes affecting lake storage.

From a management perspective, the continuous satellite-based monitoring approach developed here provides a practical framework for early detection of declining water availability. The progressive reduction observed after 2022 suggests that integrating remote sensing indicators into reservoir monitoring systems could support proactive planning before critical storage thresholds are reached. Such monitoring approaches can support adaptive lake management strategies by improving early warning capacity and informing restoration-oriented interventions under changing climatic conditions (Tammeorg et al., 2024).

Limitations and future research directions

Several limitations should be considered when interpreting the findings. First, validation of the MNDWI-based water classification relied on Sentinel-2 observations available from 2017 onwards. Consequently, classification performance for the earlier Landsat period assumes temporal consistency of spectral behaviour across different sensors and hydrological conditions. Although Collection 2 harmonization and monthly compositing reduce sensor-related uncertainties, some residual differences may remain. Second, temperature-dependent analyses were restricted to the 2005–2020 period because ERA5 temperature values before 2005 showed inconsistencies with regional climatological characteristics. Therefore, conclusions involving temperature effects should be interpreted within this reliable observation period. Third, the regression models explained 23.6–26.9% of monthly water-area variability, indicating that important processes remain unresolved. Missing variables, including reservoir operation schedules, water withdrawals, groundwater exchanges, and irrigation demands, may contribute substantially to the remaining variability. Future studies integrating these datasets could improve causal understanding. Fourth, the positive relationship between NDVI and water area should not be interpreted as evidence of vegetation-driven water increase. Additional hydrological variables, partic-

ularly evapotranspiration and soil moisture indicators, are required to evaluate vegetation–water interactions more comprehensively. Finally, the 2026 observations represent only January–April conditions and should be considered a partial-year observation rather than a complete annual record. Continued monitoring will be necessary to determine whether the observed recovery represents a temporary response or a longer-term hydrological transition. Overall, this study demonstrates that temporal completeness is a critical requirement for detecting hydrological change in Mediterranean freshwater systems. The integration of multi-decadal Landsat observations, hydroclimatic indicators, and statistical change detection provides a framework that, while validated here for a single reservoir, offers a template for assessing water-resource vulnerability in other Mediterranean freshwater systems under increasingly variable climate conditions.

Conclusions

This study provides a temporally extended assessment of Lake Belevi dynamics using 273 monthly Landsat-derived surface water observations (2000–2026), integrated with CHIRPS precipitation, ERA5 temperature, watershed-scale NDVI, SPI-based drought characterization, and statistical change detection approaches. The main conclusions are summarized as follows: (1) The complete 2000–2026 observation period revealed a statistically significant decreasing trend in monthly surface water area (Seasonal Mann–Kendall $p = 0.014$; Sen slope = −1.27 ha month^{-1}), whereas the truncated 2000–2020 record indicated an opposite increasing trend. This reversal demonstrates that temporal completeness is a critical methodological requirement for reliable hydrological trend assessment, particularly in climate-sensitive Mediterranean freshwater systems where recent extreme events may substantially modify long-term interpretations. (2) PELT change-point analysis identified five major structural transitions (2005, 2013, 2016, 2022, and 2025), demonstrating that Lake Belevi has experienced multiple hydrological regimes rather than a single monotonic trajectory. The detected phases describe a transition from relatively stable conditions to a high-storage period (2013–2016; mean 134.8 ha), followed by progressive depletion and increased hydrological variability. (3) The extreme drought event of 2025 reduced surface water extent to 4.7 ha in October 2025, representing a 96.5% decrease compared with the 2013–2016 peak period. The subsequent rapid increase to 180.7 ha in February 2026 highlights the strong sensitivity of Mediterranean freshwater systems to alternating drought and high-precipitation extremes. (4) Watershed NDVI exhibited a significant increasing trend during 2000–2025 (Mann–Kendall $p < 0.001$; +53.2%), occurring simultaneously with long-term fluctuations and decline in surface water availability. This vegetation–water divergence indicates that vegetation greening alone cannot be interpreted as evidence of improved catchment water conditions and should be evaluated together with hydroclimatic and hydrological variables. (5) Lagged hydroclimatic analyses demonstrated that precipitation and temperature influence lake dynamics through delayed responses. Maximum precipitation influence occurred at a 3-month lag ($r = 0.404$), while temperature showed the strongest negative association at a 2-month lag ($r = −0.414$), emphasizing the importance of considering temporal delays in Mediterranean catchment–lake interactions. (6) Regression modelling showed that hydroclimatic variables, particularly cumulative precipitation conditions represented by SPI-3, explain a significant but incomplete proportion of monthly water-area variability ($R^2 = 0.269$). The remaining variability likely reflects additional processes, including reservoir operation practices, groundwater interactions, and catchment-scale factors that were unavailable within the current dataset. Overall, this study demonstrates that temporally complete satellite observations combined with hydroclimatic indicators and robust statistical analysis provide an effective framework for detecting non-stationary changes in Mediterranean freshwater systems. While this study focuses on a single reservoir, the proposed framework highlights the broader importance of continuous Earth observation records for improving the reliability of hydrological change detection in climate-sensitive freshwater systems, and provides a basis for future multi-lake applications.

Statements and declarations

Acknowledgments: During the preparation of this manuscript, the author(s) used Claude and ChatGPT for the purposes of translation and language editing. The authors have reviewed and edited the output and take full responsibility for the content of this publication.

Competing interests: The authors declare no competing interests.

Ethics approval: Not applicable. This study did not involve human participants, human data, animals, or biological material; all data used were derived from publicly available satellite remote sensing and reanalysis products.

Consent to participate: Not applicable.

Consent to publish: Not applicable.

Funding: This research received no external funding.

Data availability: The Landsat Collection 2 Level-2 surface reflectance data, CHIRPS precipitation data, and ERA5 reanalysis data used in this study are publicly available through the Google Earth Engine data catalog (https://developers.google.com/earth-engine/datasets). Derived monthly surface-water-area, NDVI, and hydroclimatic time series generated during this study are available from the corresponding author on reasonable request.

Author contributions: Conceptualization, N.G., M.A. and Z.A.P.; methodology, N.G. and M.A.; software, N.G.; validation, N.G., M.A. and Z.A.P.; formal analysis, N.G.; investigation, N.G. and M.A.; resources, N.G., M.A. and Z.A.P.; data curation, N.G. and M.A.; writing—original draft preparation, N.G., M.A. and Z.A.P.; writing—review and editing, N.G., M.A. and Z.A.P.; visualization, N.G.; supervision, N.G., M.A. and Z.A.P.; project administration, N.G., M.A. and Z.A.P. All authors have read and agreed to the published version of the manuscript.

Ethical responsibilities of authors: All authors have read, understood, and have complied as applicable with the statement on "Ethical responsibilities of Authors" as found in the Instructions for Authors.

Abbreviations

AOI	Area of Interest
ANOVA	Analysis of Variance
CHIRPS	Climate Hazards Group InfraRed Precipitation with Station data
CUSUM	Cumulative Sum
ERA5	ECMWF Reanalysis v5
ET	Evapotranspiration
ETM+	Enhanced Thematic Mapper Plus (Landsat 7 sensor)
GEE	Google Earth Engine
IPCC	Intergovernmental Panel on Climate Change
JRC	Joint Research Centre
LSTM	Long Short-Term Memory (neural network)
MAE	Mean Absolute Error
MK	Mann–Kendall (test)
MNDWI	Modified Normalized Difference Water Index
MODIS	Moderate Resolution Imaging Spectroradiometer
MOD16	MODIS Global Evapotranspiration Product

569	NDVI	Normalized Difference Vegetation Index
570	NDWI	Normalized Difference Water Index
571	NIR	Near-Infrared
572	OA	Overall Accuracy
573	OLI	Operational Land Imager (Landsat 8/9 sensor)
574	OLS	Ordinary Least Squares
575	PA	Producer's Accuracy
576	PELT	Pruned Exact Linear Time (change-point detection algorithm)
577	RF	Random Forest
578	RMSE	Root Mean Square Error
579	SD	Standard Deviation
580	SLC	Scan Line Corrector (Landsat 7)
581	SPI	Standardized Precipitation Index
582	SR	Surface Reflectance
583	SWIR1	Shortwave Infrared band 1
584	TM	Thematic Mapper (Landsat 5 sensor)
585	UA	User's Accuracy
586	USGS	United States Geological Survey
587	MOD16	MODIS Global Evapotranspiration Product
588	NDVI	Normalized Difference Vegetation Index
589	NDWI	Normalized Difference Water Index
590	NIR	Near-Infrared
591	OA	Overall Accuracy
592	OLI	Operational Land Imager (Landsat 8/9 sensor)
593	OLS	Ordinary Least Squares
594	PA	Producer's Accuracy
595	PELT	Pruned Exact Linear Time (change-point detection algorithm)
596	RF	Random Forest
597	RMSE	Root Mean Square Error
598	SD	Standard Deviation
599	SLC	Scan Line Corrector (Landsat 7)
600	SPI	Standardized Precipitation Index
601	SR	Surface Reflectance
602	SWIR1	Shortwave Infrared band 1
603	TM	Thematic Mapper (Landsat 5 sensor)

UA User's Accuracy

USGS United States Geological Survey

References

Alotaibi, B. A., Baig, M. B., Najim, M. M., Shah, A. A., & Alamri, Y. A. (2023). Water scarcity management to ensure food scarcity through sustainable water resources management in Saudi Arabia. *Sustainability*, 15(13), 10648. https://doi.org/10.3390/su151310648

Anderegg, W. R. L., Trugman, A. T., Badgley, G., Anderson, C. M., Bartuska, A., Ciais, P., Cullenward, D., Field, C. B., Freeman, J., Goetz, S. J., et al. (2020). Climate-driven risks to the climate mitigation potential of forests. *Science*, 368(6497), eaaz7005. https://doi.org/10.1126/science.aaz7005

Chatfield, C., & Xing, H. (2019). *The analysis of time series: An introduction with R* (7th ed.). Chapman and Hall/CRC.

Draper, N. R., & Smith, H. (1998). *Applied regression analysis* (3rd ed.). Wiley.

Funk, C., Peterson, P., Landsfeld, M., Pedreros, D., Verdin, J., Shukla, S., Husak, G., Rowland, J., Harrison, L., Hoell, A., et al. (2015). The climate hazards infrared precipitation with stations—A new environmental record for monitoring extremes. *Scientific Data*, 2, 150066. https://doi.org/10.1038/sdata.2015.66

Gorelick, N., Hancher, M., Dixon, M., Ilyushchenko, S., Thau, D., & Moore, R. (2017). Google Earth Engine: Planetary-scale geospatial analysis for everyone. *Remote Sensing of Environment*, 202, 18–27. https://doi.org/10.1016/j.rse.2017.06.031

Hersbach, H., Bell, B., Berrisford, P., Hirahara, S., Horányi, A., Muñoz-Sabater, J., Nicolas, J., Peubey, C., Radu, R., Schepers, D., et al. (2020). The ERA5 global reanalysis. *Quarterly Journal of the Royal Meteorological Society*, 146(730), 1999–2049. https://doi.org/10.1002/qj.3803

Hirsch, R. M., & Slack, J. R. (1984). A nonparametric trend test for seasonal data with serial dependence. *Water Resources Research*, 20(6), 727–732. https://doi.org/10.1029/WR020i006p00727

Ingrao, C., Strippoli, R., Lagioia, G., & Huisingh, D. (2023). Water scarcity in agriculture: An overview of causes, impacts and approaches for reducing the risks. *Heliyon*, 9(8), e18507. https://doi.org/10.1016/j.heliyon.2023.e18507

IPCC. (2013). *Climate change 2013: The physical science basis. Contribution of Working Group I to the Fifth Assessment Report of the Intergovernmental Panel on Climate Change*. Cambridge University Press. https://www.ipcc.ch/report/ar5/wg1/

IPCC. (2023). *Climate change 2023: Synthesis report. Contribution of Working Groups I, II and III to the Sixth Assessment Report*. IPCC. https://www.ipcc.ch/report/ar6/syr/downloads/report/IPCC_AR6_SYR_FullVolume.pdf

Işıldar, H. T., & Ercoşkun, Ö. Y. (2021). Göller Yöresinde sürdürülebilirlik ve dirençlilik. *Journal of Management Theory and Practices Research*, 2(1), 89–116. https://izlik.org/JA83NL99EA

Jiménez-Bonilla, A., Rodríguez-Rodríguez, M., Yanes, J. L., & Gázquez, F. (2023). Hydrological modelling and evolution of lakes and playa-lakes in southern Spain constrained by geology, human

management and climate change. *Science of the Total Environment*, 905, 167183. https://doi.org/10.1016/j.scitotenv.2023.167183

Karimi, M., Tabiee, M., Karami, S., Karimi, V., & Karamidehkordi, E. (2024). Climate change and water scarcity impacts on sustainability in semi-arid areas: Lessons from the South of Iran. *Groundwater for Sustainable Development*, 24, 101075. https://doi.org/10.1016/j.gsd.2023.101075

Kendall, M. G., & Gibbons, J. D. (1962). *Rank correlation methods*. Griffin.

Killick, R., Fearnhead, P., & Eckley, I. A. (2012). Optimal detection of changepoints with a linear computational cost. *Journal of the American Statistical Association*, 107(500), 1590–1598. https://doi.org/10.1080/01621459.2012.737745

Kruskal, W. H., & Wallis, W. A. (1952). Use of ranks in one-criterion variance analysis. *Journal of the American Statistical Association*, 47(260), 583–621.

Mann, H. B. (1945). Nonparametric tests against trend. *Econometrica*, 13(3), 245–259. https://doi.org/10.2307/1907187

Naeem, M., Zhang, Y., Nourani, V., Tian, X., & Miao, P. (2025). Both climate and anthropogenic impacts on recent lake area change in the Erdos Plateau. *Journal of Environmental Management*, 373, 123443. https://doi.org/10.1016/j.jenvman.2024.123443

Parvaze, S., Kumar, R., Khan, J. N., & Parvaze, S. (2023). Climate change, drought, and water resources. In *Integrated drought management* (Vol. 1, pp. 541–568). CRC Press. https://doi.org/10.1201/9781003276555

Pekel, J.-F., Cottam, A., Gorelick, N., & Belward, A. S. (2016). High-resolution mapping of global surface water and its long-term changes. *Nature*, 540, 418–422. https://doi.org/10.1038/nature20584

Pınarlık, M., İbiş, A., & Selek, Z. (2023). İklim değişikliği etkisi altında Burdur Gölü su seviyesi değişimlerinin istatistiksel olarak incelenmesi. *Mühendislik Bilimleri ve Tasarım Dergisi*, 11(1), 81–93. https://doi.org/10.21923/jesd.1144586

Polat, Z. A., Memduhoğlu, A., Hacar, M., & Duman, H. (2017). Kentsel büyüme ile motorlu araç trafiği yoğunluğu arasındaki ilişkinin belirlenmesi: İstanbul örneği. *Niğde Ömer Halisdemir Üniversitesi Mühendislik Bilimleri Dergisi*, 6(2), 442–451. https://doi.org/10.28948/ngumuh.341275

Ray, R. L., & Tikuye, B. G. (2025). *Impact of climate change on surface water resources*. IntechOpen. https://doi.org/10.5772/intechopen.1011407

Sen, P. K. (1968). Estimates of the regression coefficient based on Kendall's tau. *Journal of the American Statistical Association*, 63(324), 1379–1389. https://doi.org/10.1080/01621459.1968.10480934

Sharma, K., Rajan, S., & Nayak, S. K. (2024). Water pollution: Primary sources and associated human health hazards with special emphasis on rural areas. In *Water resources management for rural development* (pp. 3–14). Elsevier. https://doi.org/10.1016/B978-0-443-18778-0.00014-3

Tammeorg, O., Chorus, I., Spears, B., Nõges, P., Nürnberg, G. K., Tammeorg, P., & Lürling, M. (2024). Sustainable lake restoration: From challenges to solutions. *WIREs Water*, 11(1), e1689. https://doi.org/10.1002/wat2.1689

Tramblay, Y., Llasat, M. C., Randin, C., & Coppola, E. (2020). Climate change impacts on water resources in the Mediterranean. *Regional Environmental Change*, 20, 83. https://doi.org/10.1007/s10113-020-01665-0

TRT Haber. (2025, July 17). Belevi Gölü, yaşanan kuraklık nedeniyle alarm veriyor. https://www.trthaber.com/foto-galeri/belevi-golu-yasanan-kuraklik-nedeniyle-alarm-veriyor/74429/sayfa-1.html

Wang, H., & Sun, Q. (2024). Urban sprawl and imbalance between supply and demand of ecosystem services: Evidence from China's Yangtze River Delta urban agglomerations. *Sustainability*, 16(19), 8269. https://doi.org/10.3390/su16188269

Wulder, M. A., Roy, D. P., Radeloff, V. C., Loveland, T. R., Anderson, M. C., Johnson, D. M., Healey, S., Zhu, Z., Scambos, T. A., Pahlevan, N., et al. (2022). Fifty years of Landsat science and impacts. *Remote Sensing of Environment*, 280, 113195. https://doi.org/10.1016/j.rse.2022.113195

Xu, H. (2006). Modification of normalised difference water index (NDWI) to enhance open water features in remotely sensed imagery. *International Journal of Remote Sensing*, 27(14), 3025–3033. https://doi.org/10.1080/01431160600589179

Xu, H., Zhang, F., Jim, C. Y., Chan, N. W., Tan, M. L., Wei, L., & Qiao, Q. (2025). Regional variations in lake areas in China due to human and natural environmental factors since 1990. *Ecological Indicators*, 172, 113307. https://doi.org/10.1016/j.ecolind.2025.113307

Yao, F., Livneh, B., Rajagopalan, B., Wang, J., Crétaux, J.-F., Wada, Y., & Berge-Nguyen, M. (2023). Satellites reveal widespread decline in global lake water storage. *Science*, 380(6646), 743–749. https://doi.org/10.1126/science.abo2812

Zhu, Z., Piao, S., Myneni, R. B., Huang, M., Zeng, Z., Canadell, J. G., et al. (2016). Greening of the Earth and its drivers. *Nature Climate Change*, 6, 791–795. https://doi.org/10.1038/nclimate3004